International Journal of Modern Agriculture
ISSN: 2305-7246
Volume 10 Issue 1, 2021

INCORPORATION AND CHARACTERIZATION OF COBALT ION DOPED HYDROXYAPATITE

K.Poovendran[1*,] K.S.Joseph Wilson[2],K.Kathiresan[3]

[1, 2] *PG and Research Department of Physics, Arul Anandar College (Autonomous), Karumathur. TN. India*

[3]. *Department of physics, PSNA College of Engineering & Technology, Dindigul – 624622, TN. India*

**E-mail: poov4u@gmail.com*

ABSTRACT --The aim of the present work is to investigate the doping effect of Cobalt (Co) metal ions with hydroxyapatite (HAp). The Cobalt was doped at four different concentrations such as 0.2, 0.4, 0.6, and 0.8 mole with HAp (namely Co-HAp) were synthesized by a wet chemical precipitation method. The synthesized pure sample (green) of Co doped HAp and calcinated at 300°C of Co doped HAp samples were characterized by XRD, FTIR, SEM, EDAX,TEM and vibration sample magnetometer (VSM). The Co doped HAp, a bio ceramic powder can be helpful in the replacements of hips, knees, teeth, tendons and ligaments, as well as repair for periodontal disease, maxillofacial reconstruction, augmentation and stabilization of the jawbone, spinal fusion and bone fillers after tumour surgery.

I. INTRODUCTION

Hydroxylapatite is the main inorganic component of human bones and teeth. As a material, gratitude to its high-quality properties of Bio-compatibility, bioactivity and biodegradability, Fortunately, the ions of pure HAp can be artificially replaced by other cations or anions. Doped metal ions Cu2+,Zn2+ ,Fe3+/2+ , Sr2+ can offer antibacterial properties, formation of various proteins, nucleic acids in human body. Magnetic nanoparticles have received much attention, recently, because of their possible applications in the fields of biomedicine[1-3].In the middle of these applications, they are used as imaging technology, hyperthermia treatment of cancer and as magnetically targeted drug delivery agents.In its natural state, many studies have looked at placing of ferrites into the HAp. Some authors found that the insertion of the spinal ferrite MnFe2O4 through a wet chemistry process resulted in nanoparticles having a core–shell structure of HAp. It was shown that the Co2+ ions substituted into the Ca2+ sites which were nine-fold coordinated (Ca(1)sites). In these applications, the nanoparticles must be introduced into the bloodstream. This brings up the issue of the biosafety of the nanoparticles. Passivation of the surface of the magnetic nanoparticles is used to increase the Biocompatibility of these nanoparticles. [4-10]. The mechanism of the Co-HAp for PMS activation was investigated by quenching experiments and EPR analysis. The catalytic effect of hydroxyl

group on PMS activation for RhB degradation was understood via ATR-FTIR and XPS analysis. The pathway of RhB degradation in the Co-HAp activated PMS process was also understood [11].Among various types of nanomaterials, magnetic nanoparticles have attracted a great deal of attention in biomedicine and clinical applications owing to their prominent advantages such as super paramagnets, low toxicity.Moreover, magnetic nanoparticles can be conducted by an external magnetic field, providing the guided delivery of drugs and biomolecules. In addition, magnetic fields can immobilize and separate magnetically tagged biological entities.However, in practical applications, some drawbacks limit the exploitation of bare magnetic nanoparticles in the biomedical field, namely their poor chemical stability, high aggregation propensity, low adsorption drug capacity, poor release rate, and short retention time in the bloodstream. To address these grand issues, some effective protection strategies have been taken into account and made the use of these materials feasible. For instance, the grafting of small biomolecules like surfactants, the encapsulation within polymers such as dextran or chitosan, and the coating with inorganic materials such as silica and ceramics not only provide chemical stability and retard the oxidation of nanoparticles but also render the magnetic nanoparticles nontoxic and non immunogenic[12]. Recently, an intensive research has been carried out on the synthesis of mesoporous hydroxyapatite owing to its several alternative features such as high surface area, tunable pore size, and high pore volume. These features not only enhance the loading capacity and tune the release of several pharmacy molecules, but also increase the bioactivity properties of nanoparticles with respect to bone cells and tissues. Therefore, mesoporous magnetic hydroxyapatite (MMHAp) would be an excellent candidate in biomedical applications, particularly in targeted drug delivery systems. Thanks to its high drug adsorption capacity, ability to specifically target tumor cells, and to easily recover excess or unused drugs by an external magnetic field. In general, several synthesis routes have been developed to date for the fabrication of magnetic hydroxyapatite nanocomposites [13].Precisely, internalized magnetic nanoparticles cause a tensile force inside neurons by an external magnetic field, leading to the neurite and axon elongation in a particular direction. More recently, it has been reported that the combinational effect of a magnetic field and cellular uptake of BSA-coated magnetic nanoparticles lead to a higher intracellular concentration of nanoparticles. [14].

II. MATERIALS AND METHODS

The Cobalt-doped hydroxyapatite (Co–HAp) powder is equipped by a wet chemical precipitation method using calcium nitrate,ammonium dihydrogen orthophosphate and cobalt nitrate. CoHAp is prepared as a solution by taking 10-X moles of calcium nitrate dissolved with appropriate demineralised water such that the pH value of this precipitate is to be maintained between 10 and 12 by using ammonia solution. Here calcium atoms are replaced with copper atoms [(Ca10-X(PO4)6(OH)2 X = 0.2, 0.4, 0.6, 0.8 mol)]. Ammonium dihydrogen Orthophosphate solution is prepared by taking 6 mol of ammonium dihydrogen orthophosphate by properly mixed with demineralized water and ammonia is added to maintain the same pH value. Ammonium dihydrogen orthophosphate solution is added drop wise into the calcium nitrate and cobalt nitrate solution at a temperature of 60 °C. The synthesis is carried out at a molar ratio of Ca/P equal to 1.67, the incurred mother

liquor precipitate is aged, rinsed with distilled water, dried, and converted into powders using agate pestle mortar grinding.

III. RESULTS AND DISCUSSION

3.1XRD Analysis

Fig. 5.1(a-d) shows the XRD pattern of Co doped HAp powder was synthesized by co-precipitation method. The standard diffraction peaks show the hexagonal structure of Co doped HAp (Space group: P63). This is also confirmed by the JCPDS data (Card no. 9-0432). The size of the crystallite was calculated using Scherrer's equation found to be in the range 10 – 100 nm for all samples. The noises found in the XRD spectra as seen in Fig. 5.1(a–d), may be the reason for adding ammonia solution for maintaining pH value. The calculated particle size, lattice parameter and volume of Co doped HAp green samples as seen in the Table-5.1.

Fig. 5.2 (a-d) shows the XRD pattern of Co doped HAp calcinated at 300°C. All the peaks were sharp and well-differentiated shows an increase in crystalline nature and the size of the crystallite was obtained in the range 10 – 100 nm for all calcinated samples. Thecalculated particle size, lattice parameter and volume of calcinated Co doped HAp samples as seen in the Table- 5.1.

3.2FTIR Analysis

FTIR spectra of Co doped HAp and calcinated Co doped HAp samples at 300°C are shown in Fig. 5.3(a-d) and 5.4(a-d) respectively. The key characteristic peaks of all Co doped HAp samples were seen. Notably the characteristic bands were observed around 550, 640 and 960 cm−1 due to O-P-O bending mode in the phosphate groups and triply degenerate ν4 phosphate groups. Further, the bands appeared around 1400 cm−1 and 1600 cm−1 due to carbonate groups. The carbonate is a common impurity atom during synthesis of hydroxyapatite. The weak bands were observed at 3160 cm−1 and broad band at 3500cm−1 due to the presence of water in the Co doped HAp synthesized samples. In Fig. 5.4 (a-d), the calcinated samples shows an intense and sharp bands around 960 and 3500 cm−1 due to presence of phosphate and water (PO43-)in Co-HAp. All the OH, CO, PO values of green and calcinated Co doped HAp as seen in the Table 3.2.EDAX Analysis

The EDAX spectra of green and calcinated Co doped HAp are shown in Fig. 5.5(a-d). From the EDAX analysis, the component such as Ca, Co, P and O were present in green and calcinated Co doped HAp. Earlier reported results showed that the traces of Mg, Si, and Na, present during synthesis of Hap [15]. However, in our present studies the EDAX analysis shows the absence of impurities such as Mg, Si, and Na in all the samples due to the effect of calcinations at 300°C. Further, the molar ratio was calculated from the integrated intensities of Ca and P spectra found as 1.68 which is very close to standard ratio of 1.67 [16].

3.3SEM ANALYSIS Fig. 5.6(a-d) shows that SEM images of Co doped HAp samples calcinated at 300°C. All the prepared samples were grinded using mortar and pestle. The irregular shaped agglomeration images were formed as result of Co doped HAp.

3.4TEM Analysis

Fig. 5.7(a-d) shows the core/shell and needle shaped (dark ash colour shades) structure as seen in TEM images of Co doped HAp green samples. The core/shell and needle shaped

structure indicates that Co2+ is in the dominant oxidation state. Using TEM images, the size of the particle found was approximately 50-100nm for Co doped HAp green samples.

3.5 vibration sample magnetometer (VSM)

Cobalt doped HAp spectra were shown in Fig. 5.8(a-d).Usually,inthecaseofnon-stabilizedmagnetiteobtainedinaqueous mediumthereisacontinuousrowbetweenunoxidizedmagnetiteinthe NPs volume and completely oxidized to maghemite on NP surface.This way in the case of bare CoHAp sample we probably have the magnetite crystalline core (we see it in a XRD pattern) and a diffuse semi-crystalline layer consisting of gamma oxide and alpha oxyhydr- oxide. This assumption will be discussed below.For 0.4Co 9.6Ca and 0.8Co 9.2Ca the S4 sextet gone whichindicatesanroughlycompleteevolutionofoxyhydroxidetooxide afterHTT.So we can resume that the core is magnetite, whose surface Cobalt(II) atoms are oxidized to Cobalt (III), which leads to the appearance of a semi-crystallinemoreandmorediffuselayersofgammaoxideandthen alpha oxyhydroxide. Under the first synthetic stage (basic pH, air atmosphere) the intermediate layer maybe getting bigger and its presence helps the diffuse HAp shell to form. At the second stage, during HHT, crystallization of the shell and the intermediate layer occurs, whichleadstotheappearanceofintensepeaksfromironoxide.For all the samples changes of hyperfine parameters and redis- tribution of relative areas of magnetic sextets in compare with core sample were demonstrated. This could be due to the fact that the HHT and the interaction between the core surface and the structure of the formed shell lead to the formation of an intermediate magnetic layer. This fact is in a good agreement with magnetite crystallite sizes, calculated out of XRD data, which increase after shell production up to 10–60 nm, the higher is HTT temperature, the greater is crystallite size.

IV. CONCLUSION

The Cobalt was doped at four different concentrations namely, 0.2, 0.4, 0.6, and 0.8 mole with HAp synthesized by a wet chemical precipitation method. The synthesized pure sample (green) of Co doped HAp and calcinated at 300°C of Co doped HAp samples were characterized by XRD, FTIR, SEM, EDAX, and TEM. XRD result confirmed that the synthesized Co doped HAp form was hexagonal. The size of the crystallite was estimated in the range 10 – 70 nm for all samples. FTIR spectra of Co doped HAp and calcinated Co doped HAp samples shows the characteristic bands were observed around 550, 640 and 960 cm−1 due to O-P-O bending mode in the phosphate groups and triply degenerate ν4 phosphate groups. The EDAX analysis of green and calcinated Co doped HAp samples exhibits the presence of Ca, Co, P and O in all samples. SEM results show irregular shaped agglomeration images. TEM images exhibits core/shell and needle shaped structure that indicates Co2+ is in the dominant oxidation state. Using TEM images, the size of the particle found was approximately 50-100nm for Co doped HAp green samples.The saturation magnetization of core–shell NPs is linearly decreasing with the increase of HAp amount from 68 emu/g to 52 emu/g (0.2 Co 9.8HAp).

V. REFERENCE

1. Gaoyu Chen et al., RSC Adv., 2017, 7, 56537–56542.
2. V. Uskokovi´c, M. A. Iyer and V. M. Wu, J. Mater. Chem. B, 2017, 5, 1430–1445.
3. A.K. Gupta, M. Gupta, J of Biomaterials 26 (2005) 3995.
4. N. Petchsang et al. Journal of Magnetism and Magnetic Materials 321 (2009) 1990–1995.
5. H. Ohgushi, A.I. Caplan, J. Biomed. Mater. Res. (Appl. Biomater.) 48 (1999) 913.
6. D.M. Dabbs, I.A. Aksay, Annu. Rev. Phys. Chem. 51 (2000) 601.
7. D. Arcos, J. Rodrı´guez-Carvajal, M. Vallet-Regı´, Chem. Mater. 16 (2004) 2300.
8. T. Kawasaki, K. Ikeda, S. Takahashi, Y. Kuboki, Eur. J. Biochem. 155 (1986) 249.
9. M. Jiang, J. Terra, A.M. Rossi, M.A. Morales, E.M. Baggio saitovitch, D.E. Ellis, Phys. Rev. B. 66 (2002) 224107.
10. E.M. Yahiaoui, R. Berger, Y. Servant, J. Kliava, L. Cˇ ugunov, A. Mednis, J. Phys.: Condens. Matter. 6 (1994) 9415.
11. Yixiong Pang, Lingjun Kong, Diyun Chen, Gutha Yuvaraja, Sajid Mehmood. J.jhazmat.2019.121447.
12. A. Izadi, et al. J.Materials Science & Engineering C 101 (2019) 27–41.
13. S. Mondal, P. Manivasagan, S. Bharathiraja, M. Santha Moorthy, H.H. Kim, H. Seo, K.D. Lee, J. Oh, J. Nanomedicine 12 (2017) 8389–8410.
14. E. Zhang, M.F. Kircher, M. Koch, L. Eliasson, S.N. Goldberg, E. Renström, J. ACS Nano 8 (4)(2014) 3192–3201.
15. D.J.A. Netz et al: International Journal of Pharmaceutics 213 (2001) 117–125.
16. Sergey V. Dorozhkin. J. Biomaterials 31 (2010) 1465–1485.

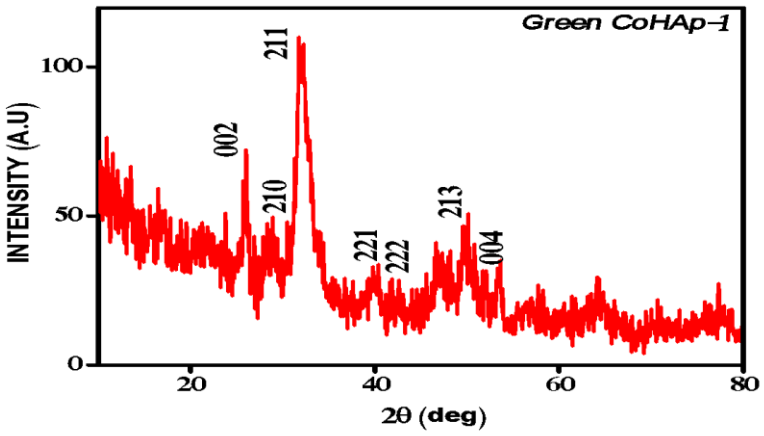

Figure 5.1a XRD image of CoHAp-1

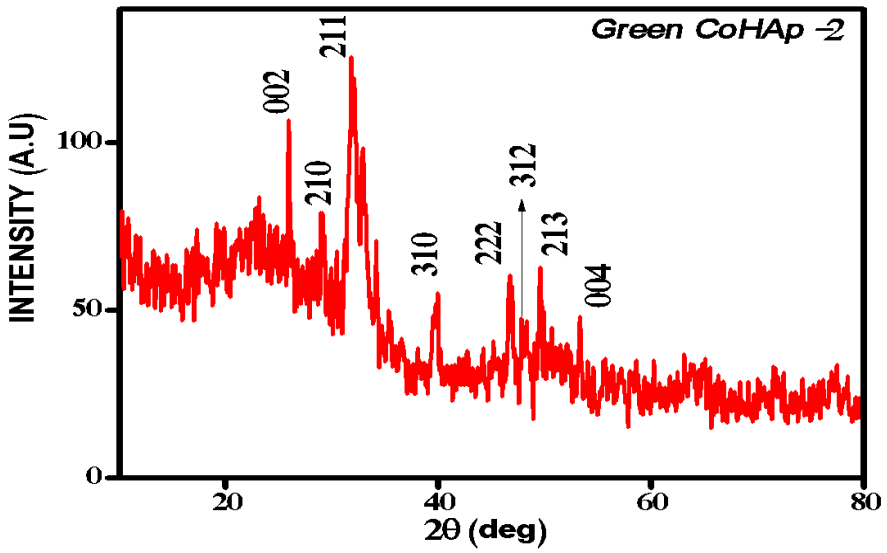

Figure 5.1bXRD image of CoHAp-2

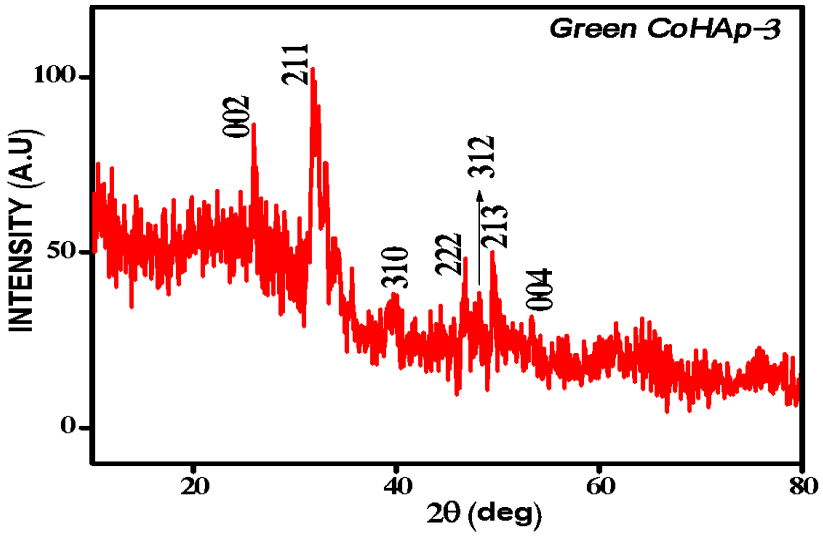

Figure 5.1cXRD image of CoHAp

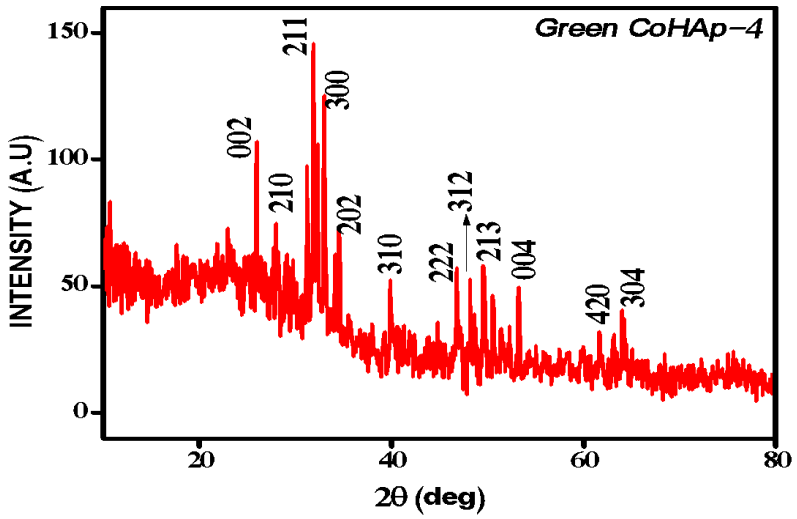

Figure 5.1dXRD image of CoHAp-4

5.2 XRD results for calcinated Samples

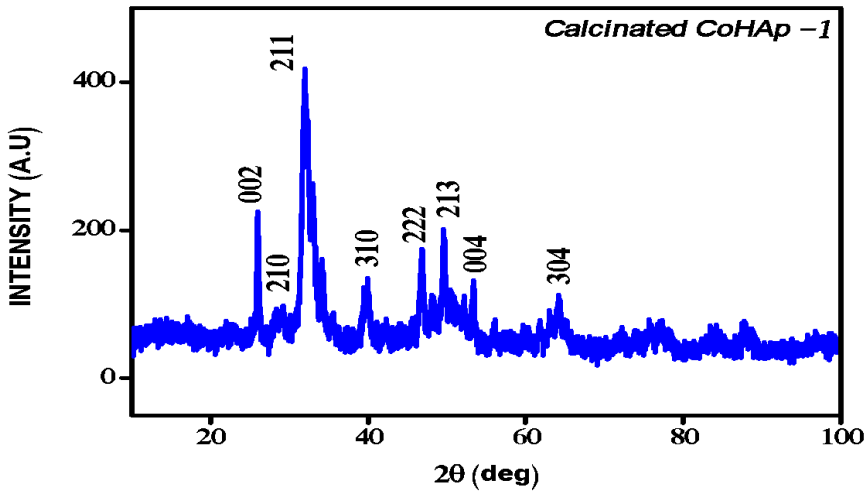

Figure 5.2a XRD image Calcinated of CoHAp-1

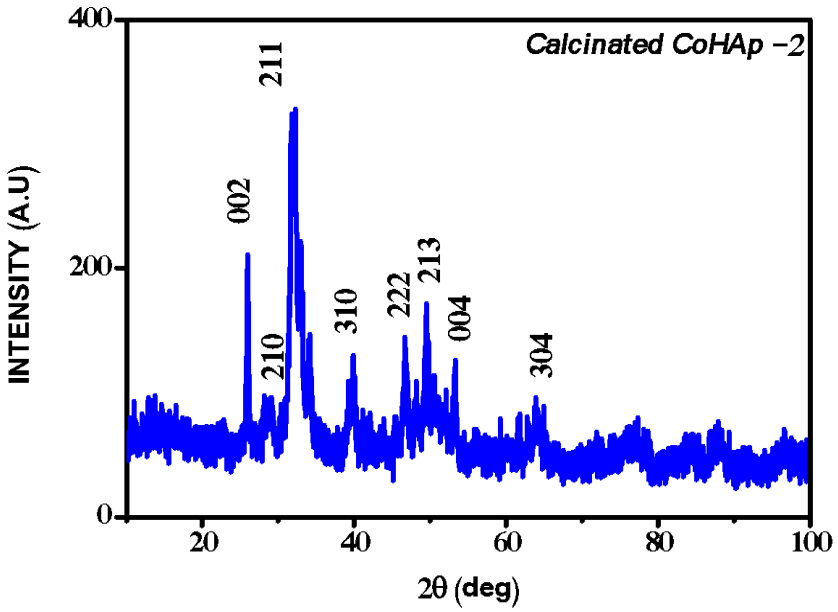

Figure 5.2b XRD image Calcinated of CoHAp-2

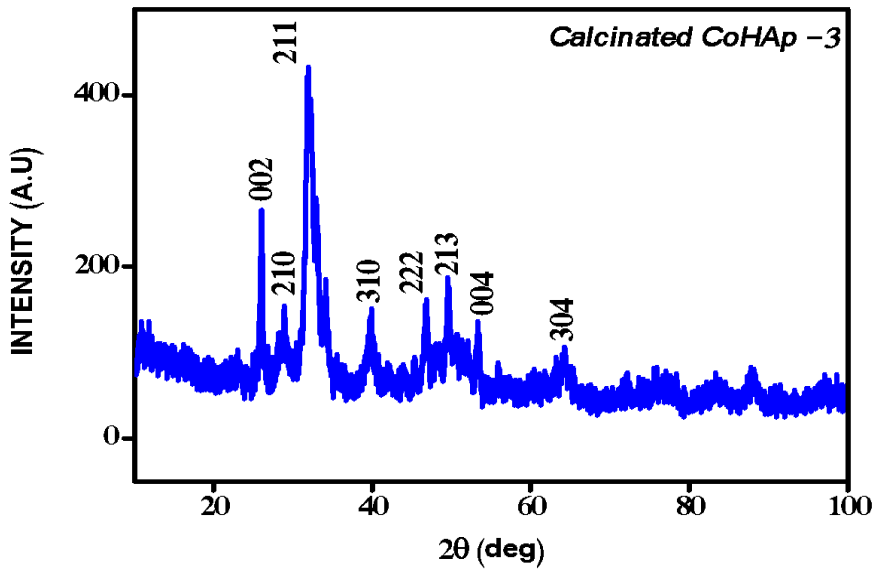

Figure 5.2c XRD image Calcinated of CoHAp-3

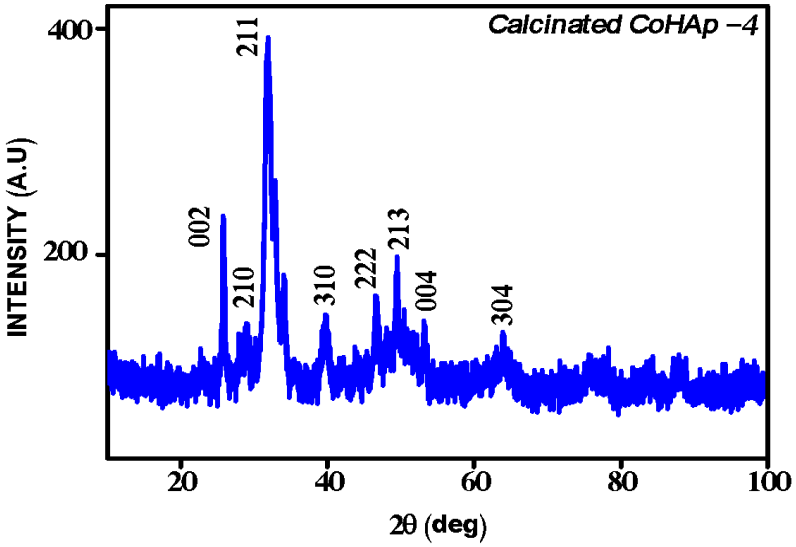

Figure 5.2dXRD images Calcinated of CoHAp-4

5.3 FTIR results for Green Sample

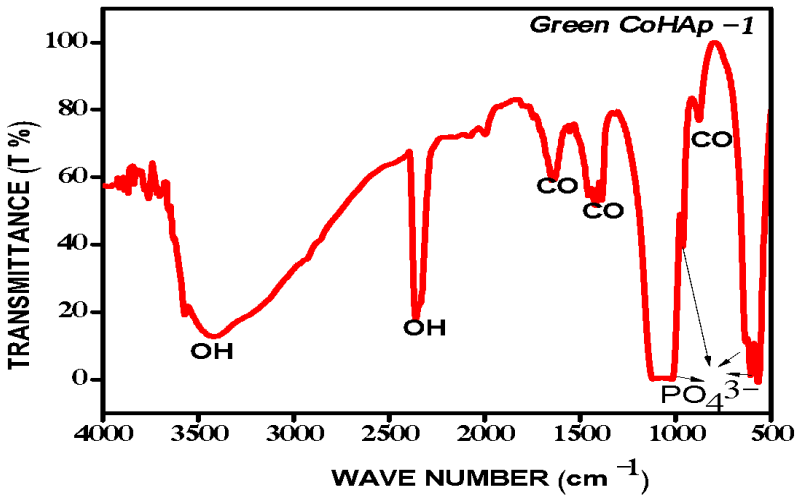

Figure 5.3a FTIR image of CoHAp-1

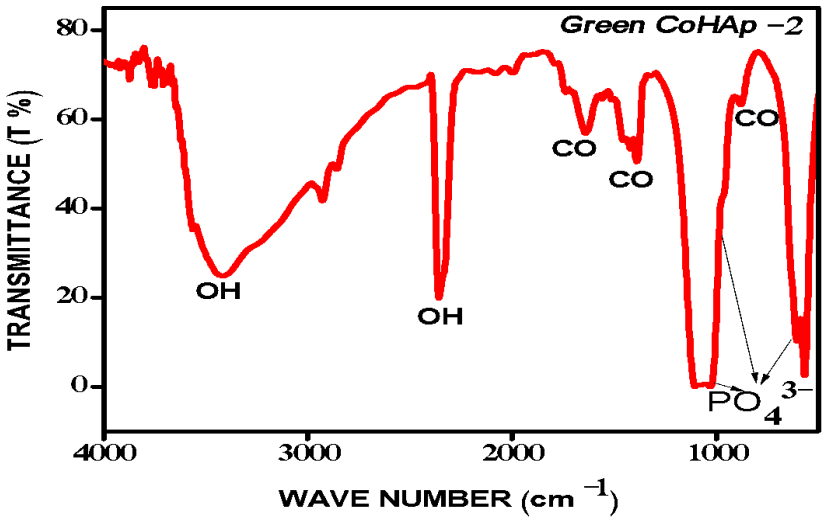

Figure 5.3b FTIR image of CoHAp-2

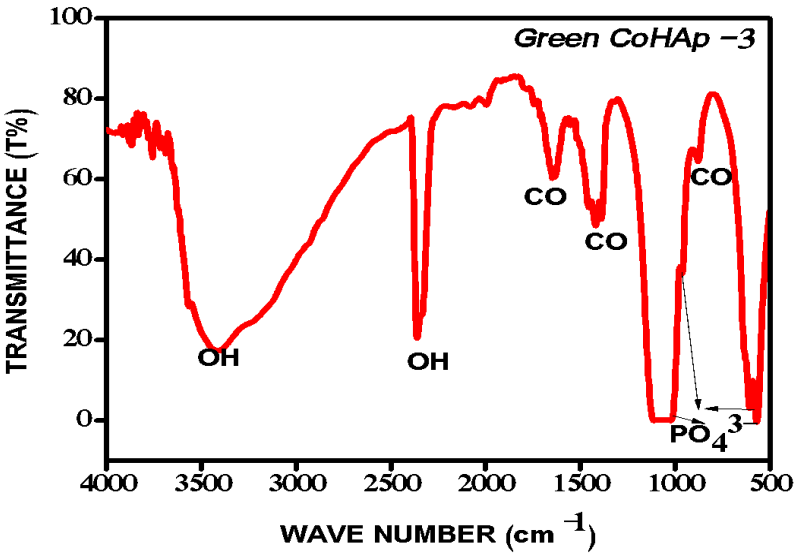

Figure 5.3c FTIR image of CoHAp-3

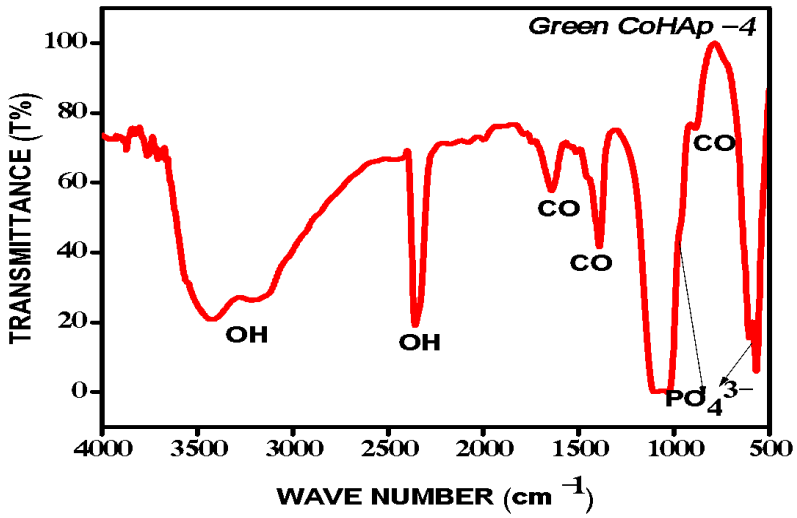

Figure 5.3dFTIR image of CoHAp-4

5.4 FTIR results for calcinated Samples

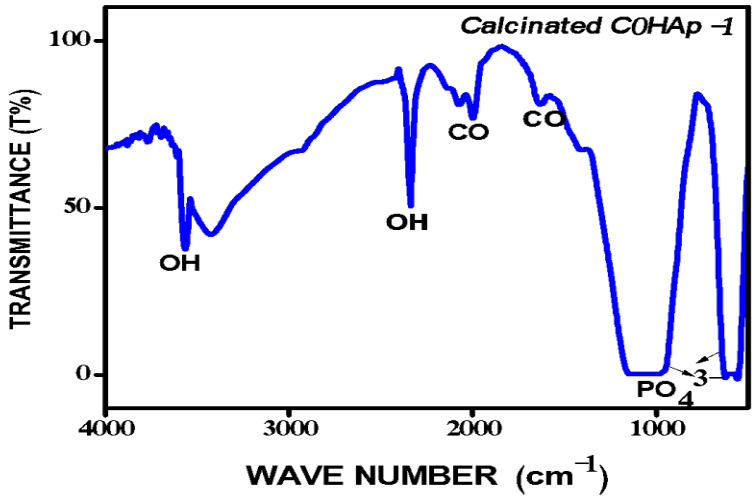

Figure 5.4a FTIR image of Calcinated CoHAp-1

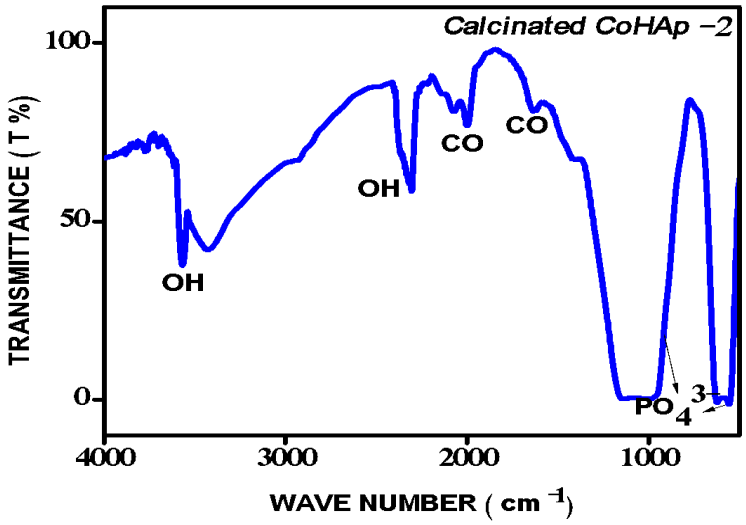

Figure 5.4bFTIR image of Calcinated CoHAp-2

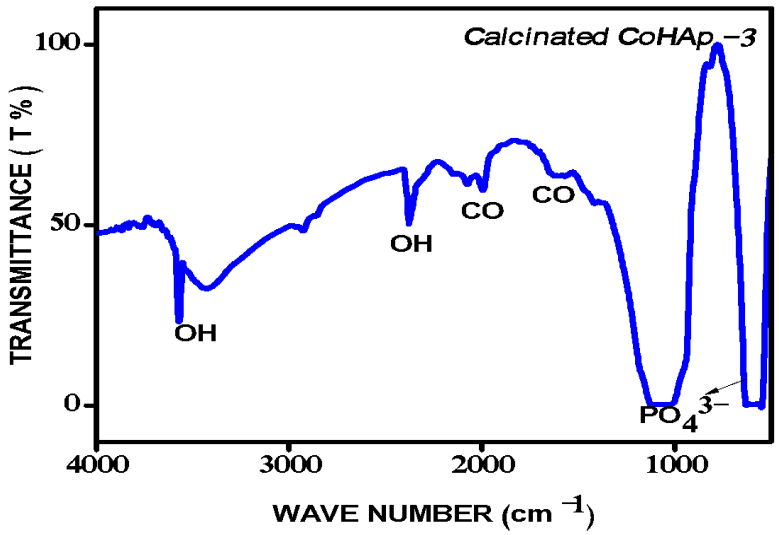

Figure 5.4c FTIR image of Calcinated CoHAp-3

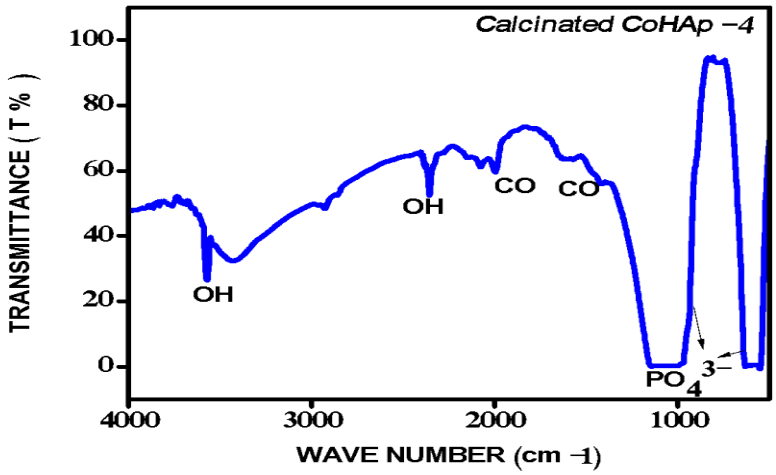

Figure 5.4d FTIR images of Calcinated CoHAp-4

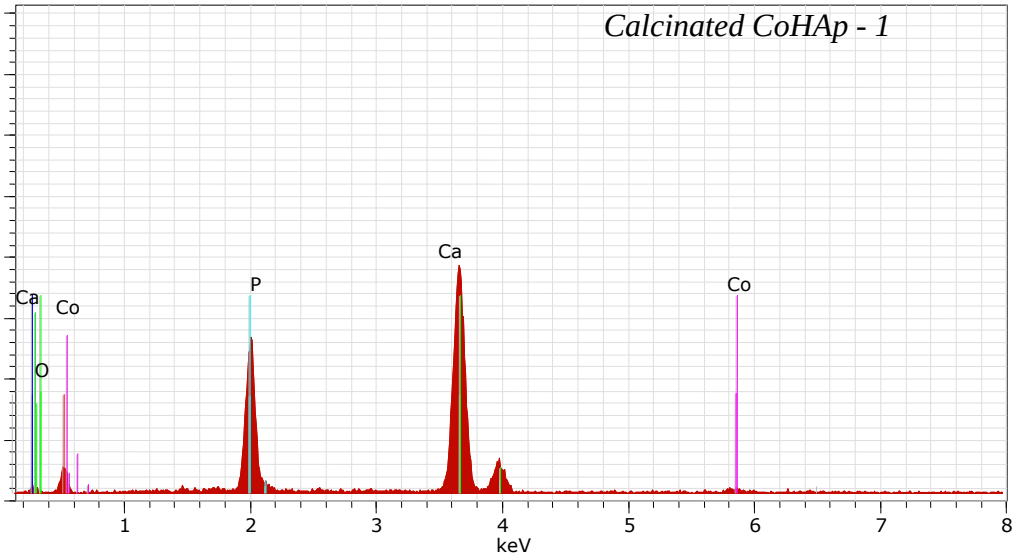

Fig. 5.5a: EDAX image of Calcinated CoHAp-1

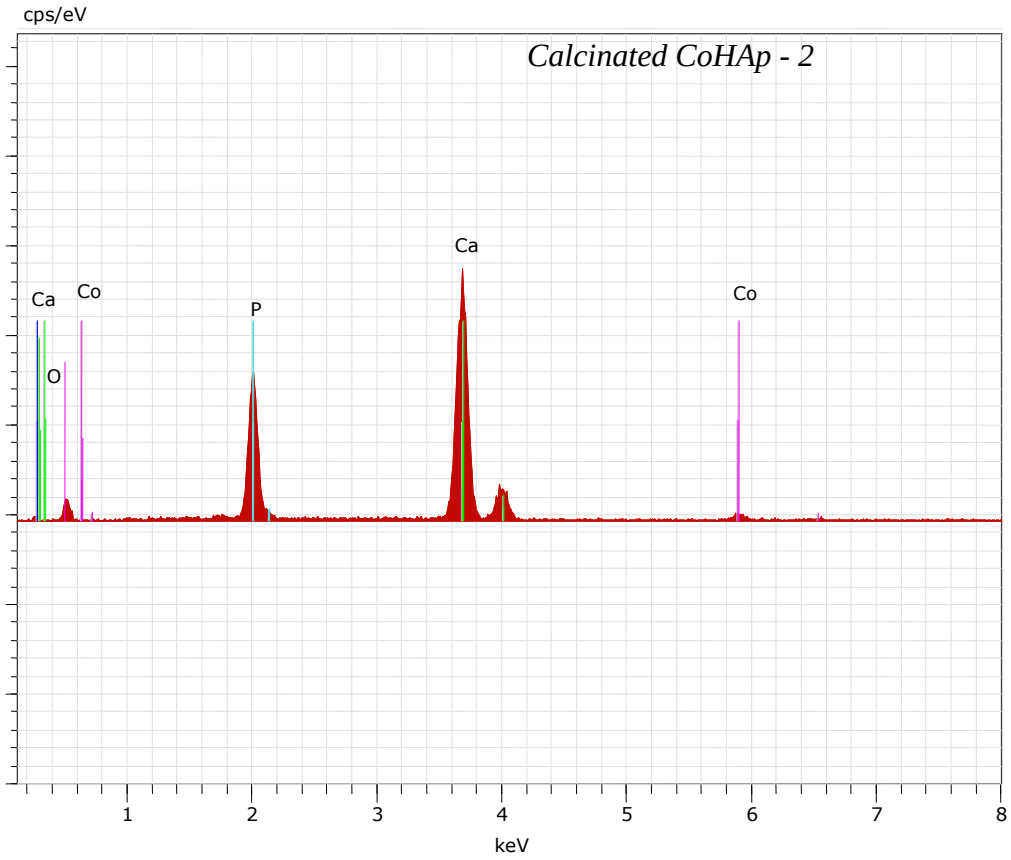

Figure 5.5b: EDAX image of Calcinated CoHAp-2

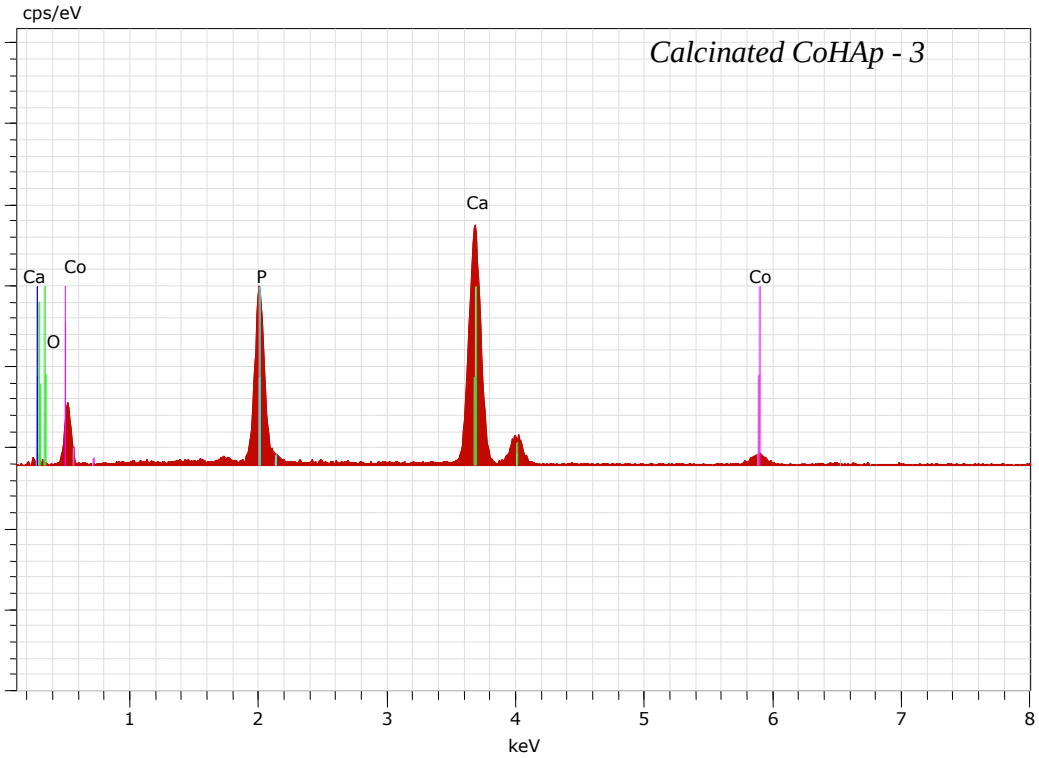

Figure 5.5c EDAX image of Calcinated CoHAp-3

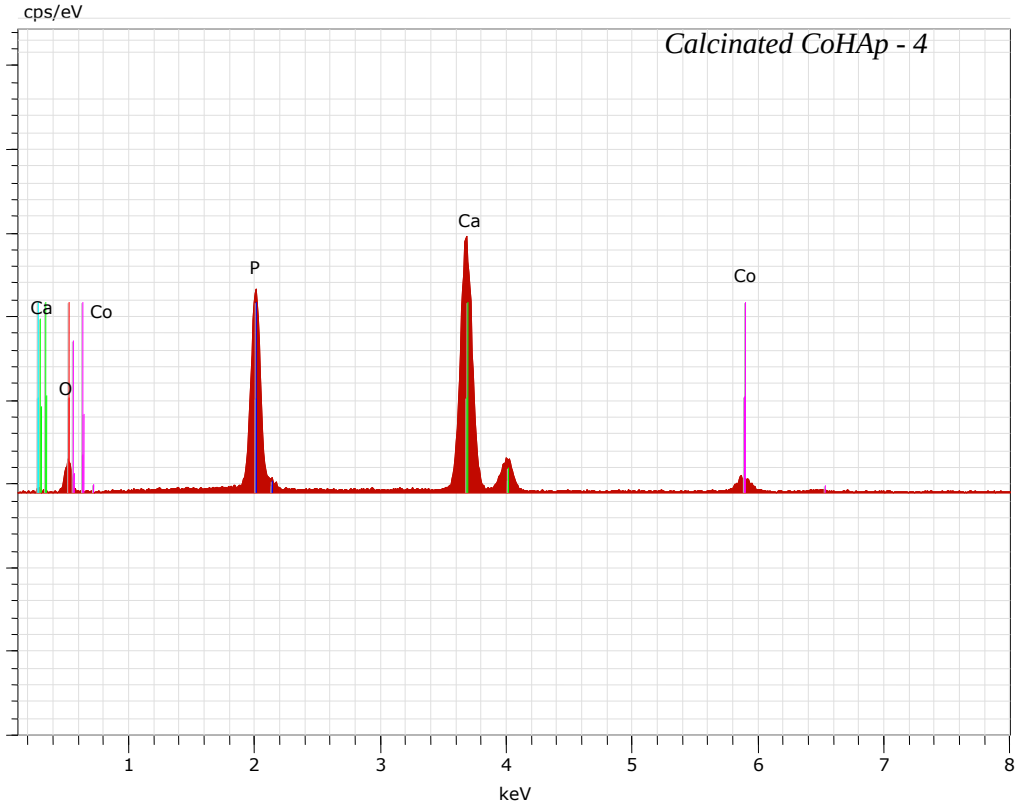

Figure 5.5EDAX image of Calcinated CoHAp-4

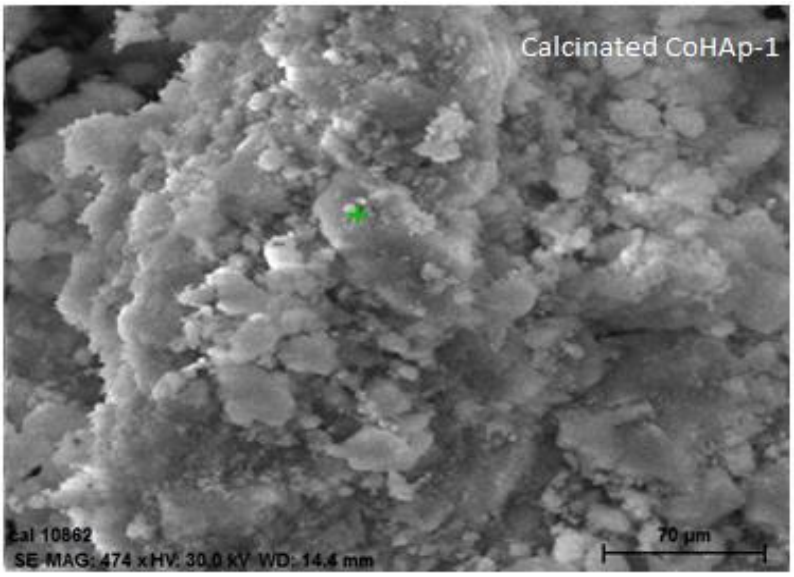

Figure 5.6aSEM image of Calcinated CoHAp-1

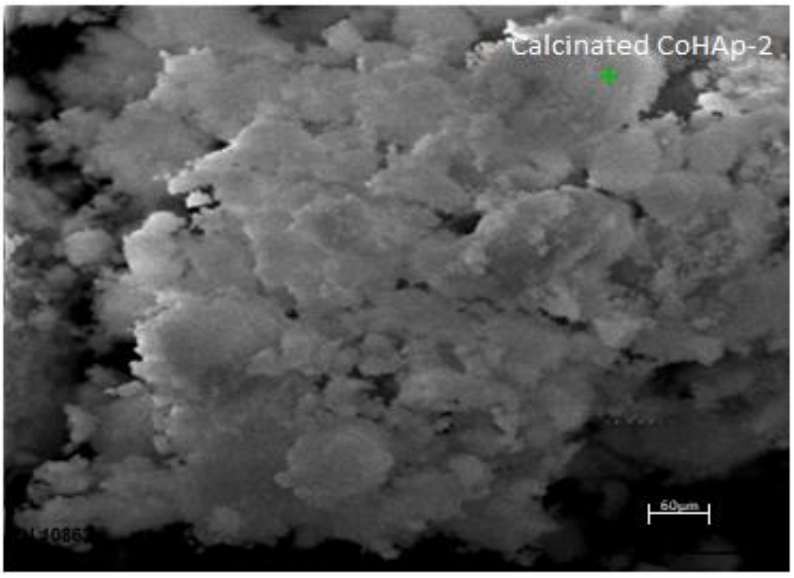

Figure 5.6b SEM image of Calcinated CoHAp-2

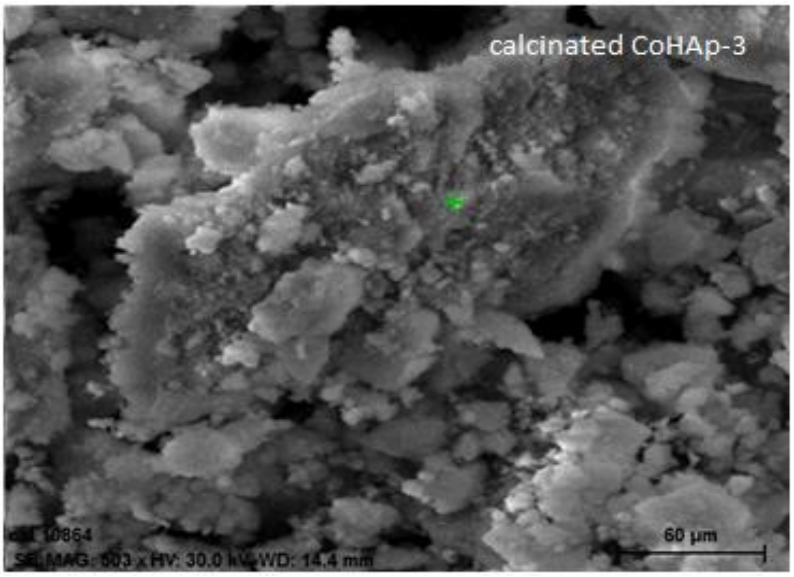

Figure 5.6cSEM image of Calcinated CoHAp-3

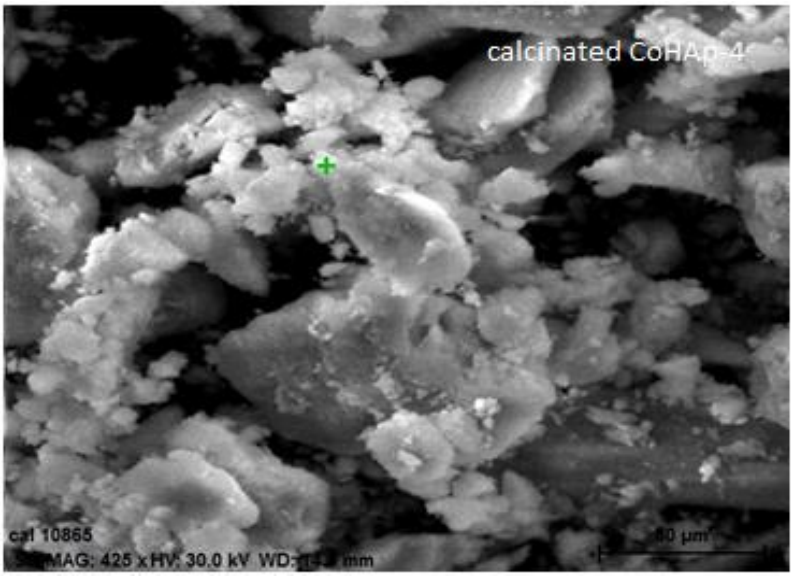

Figure 5.6d: SEM image of Calcinated CoHAp-4

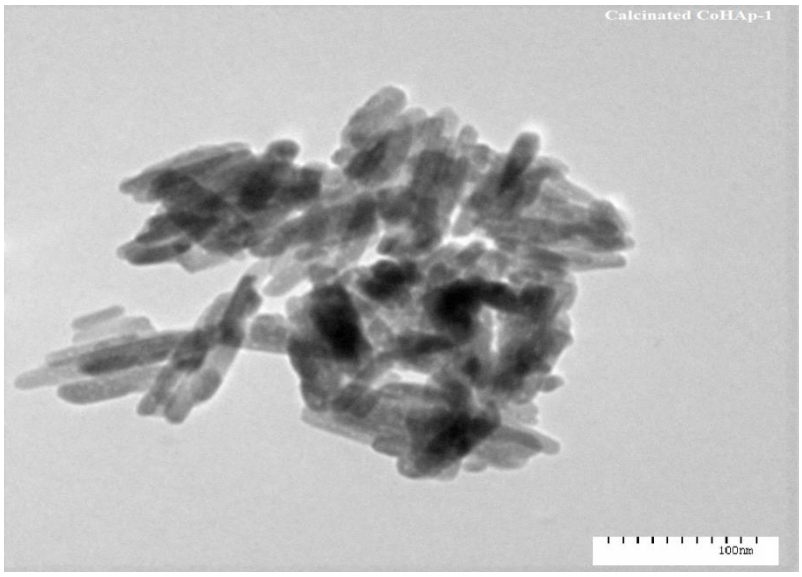

Figure 5.7aTEM image of Calcinated CoHAp-1

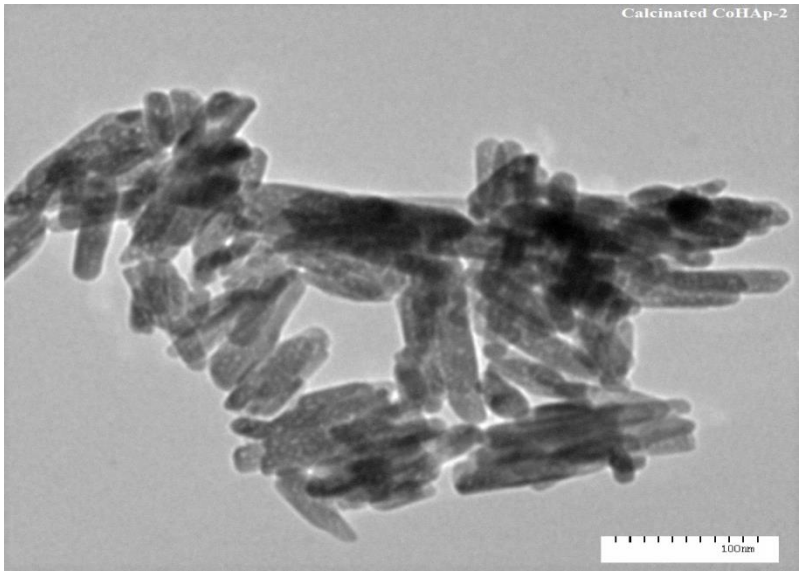

Figure 5.7b TEM image of Calcinated CoHAp-2

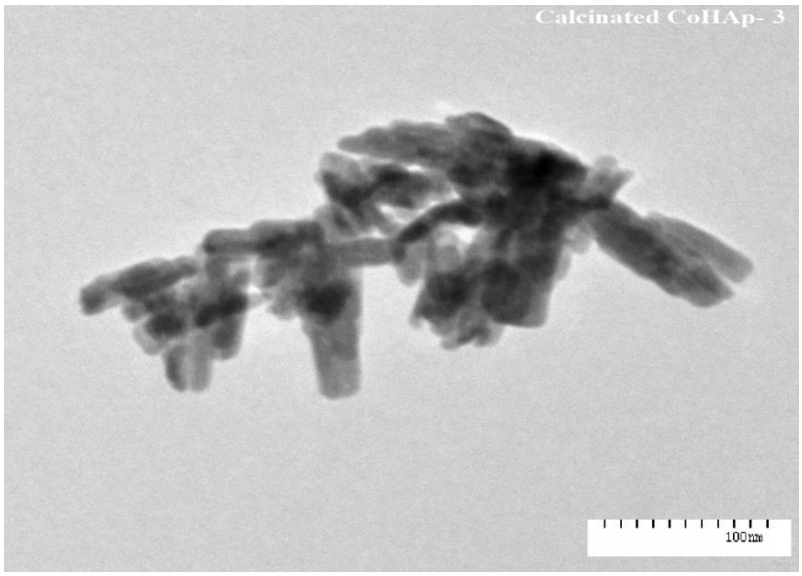

Figure 5.7cTEM image of Calcinated CoHAp-3

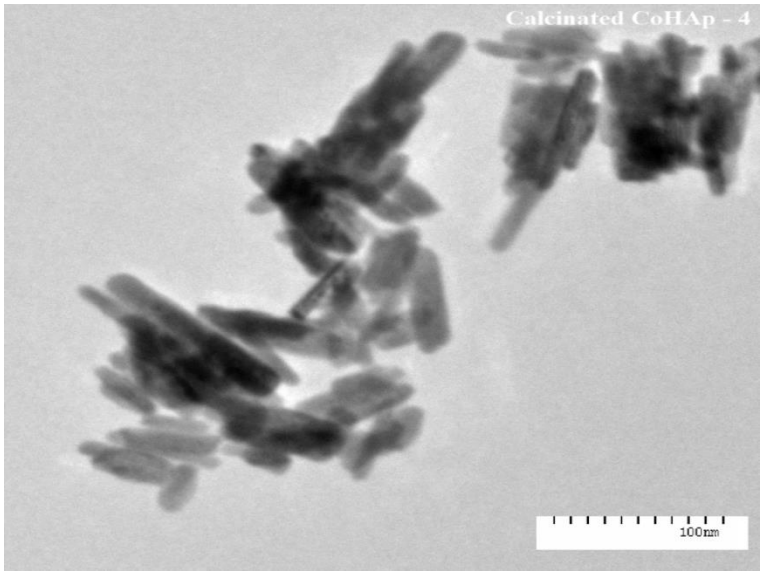

Figure 5.7d TEM image of Calcinated CoHAp-4

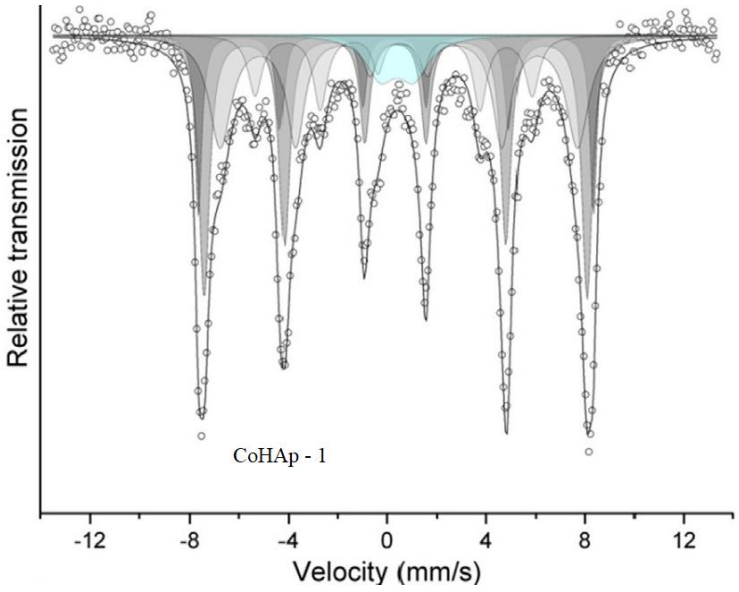

Figure 5.8a VSM image ofCoHAp-1

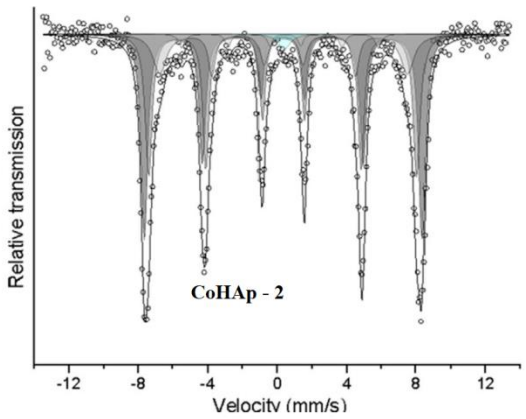

Figure 5.8b VSM image ofCoHAp-2

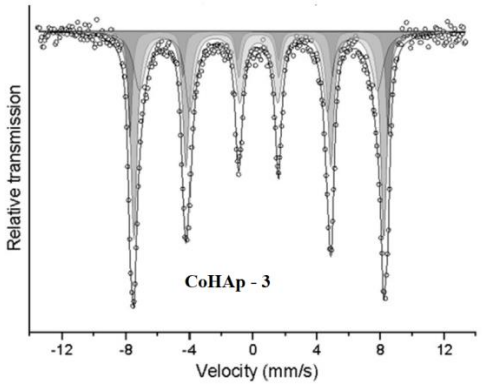

Figure 5.8c VSM image ofCoHAp-3

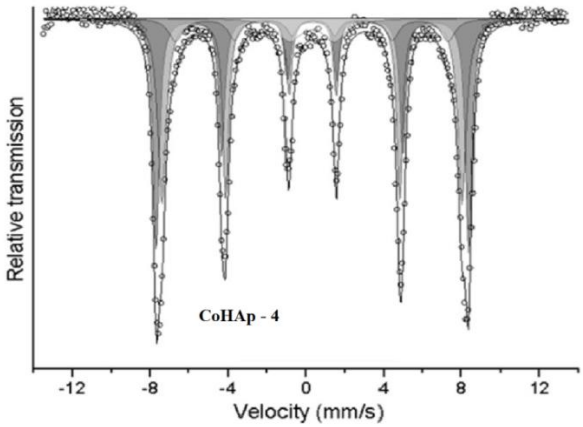

Figure 5.8d VSM image ofCoHAp-4

S.no	Description	Green Sample (Co-HAp)				Calcined Sample (Co-HAp)			
		1	2	3	4	1	2	3	4
1	Position 2ɵ	31.725	31.963	31.806	31.976	31.855	31.824	31.821	31.756
2	Particle Size - d	21.915	11.956	29.23	18.809	58.461	43.837	58.450	58.360

3	Intensity (211)	Std	100	100	100	100	100	100	100	100
		Obs	100	72.26	100	100	100	99.08	99.10	100
4	A (å)		9.4442	9.3471	9.1882	9.2430	9.0957	9.4809	9.1958	9.2776
5	C (å)		6.8414	6.7984	6.8110	6.7972	6.8074	6.4180	6.6680	6.5586
6	Volume		531.3903	554.9838	553.2940	531.4821	530.7613	554.0643	552.8431	530.7237

Table 5.1 Particle Size, Lattice Parameter and Volume of Green And Calcinated CoDoped HAp

Functional groups	Wave number (cm^{-1})							
	CoHAp - 1		CoHAp - 2		CoHAp - 3		CoHAp - 4	
	Green	Calcinated	Green	Calcinated	Green	Calcinated	Green	Calcinated
OH	3580.96	3551.42	3420.81	3556.73	3419.25	3580.96	3421.59	3568.30
C=O	1415.03	1435.25	1374.61	1639.49	1442.24	1614.83	1394.82	1606.7
$PO_4^{3-/}$	646.15	646.15	605.73	630.72	604.17	626.72	616.61	646.15

Table 5.2 Functional Groups of Green and Calcinated Co Doped HAp

Sample name	Calcium (Ca)(mol)	Cobalt (Co) mol	Phosphate (P)	(Ca+Co)/P
	atom (at %)	atom (at %)	atom (at %)	Ratio
CoHAp - 1	18.26	0.20	10.98	1.68

CoHAp - 2	14.33	0.26	8.8	1.66
CoHAp – 3	22.59	1.04	14.01	1.68
CoHAp - 4	15.21	0.48	9.53	1.65

Table 5.3 Ratio of the Ca, Co, and Phosphate using EDAX

Results of Green andCalcinated Co Doped HAp